Chapter 8
Metal Ion-Dependent DNAzymes and Their Applications as Biosensors

Tian Lan and Yi Lu

Contents

T. Lan
Department of Biochemistry, University of Illinois at Urbana-Champaign, Urbana, IL 61801, USA

Y. Lu (✉)
Department of Biochemistry, University of Illinois at Urbana-Champaign, Urbana, IL 61801, USA, and

Department of Chemistry, University of Illinois at Urbana-Champaign, Urbana, IL 61801, USA
e-mail: yi-lu@illinois.edu

A. Sigel, H. Sigel, and R.K.O. Sigel, *Interplay between Metal Ions and Nucleic Acids*, Metal Ions in Life Sciences 10, DOI 10.1007/978-94-007-2172-2_8,

Abstract Long considered to serve solely as the genetic information carrier, DNA has been shown in 1994 to be able to act as DNA catalysts capable of catalyzing a trans-esterification reaction similar to the action of ribozymes and protein enzymes. Although not yet found in nature, numerous DNAzymes have been isolated through *in vitro* selection for catalyzing many different types of reactions in the presence of different metal ions and thus become a new class of metalloenzymes. What remains unclear is how DNA can carry out catalysis with simpler building blocks and fewer functional groups than ribozymes and protein enzymes and how DNA can bind metal ions specifically to perform these functions. In the past two decades, many biochemical and biophysical studies have been carried out on DNAzymes, especially RNA-cleaving DNAzymes. Important insights have been gained regarding their metal-dependent activity, global folding, metal binding sites, and catalytic mechanisms for these DNAzymes. Because of their high metal ion selectivity, one of the most important practical applications for DNAzymes is metal ion detection, resulting in highly sensitive and selective fluorescent, colorimetric, and electrochemical sensors for a wide range of metal ions such as Pb^{2+}, UO_2^{2+}, including paramagnetic metal ions such as Cu^{2+}. This chapter summarizes recent progresses in *in vitro* selection of metal ion-selective DNAzymes, their biochemical and biophysical studies and sensing applications.

Keywords biosensor • catalysis • DNA • DNAzyme • metalloenzyme • metal sensing

1 Introduction

For a long time, DNA's only function was perceived as being the genetic material for all organisms. The genetic information is encoded by certain combinations of the four nucleobases: adenine (A), thymine (T), guanine (G), and cytosine (C). Because of the limitation of functional group diversity in the building blocks of DNA in comparison with other biomolecules such as proteins, and because of the mostly invariant double helical structure, DNA was considered to be incapable of catalyzing chemical reactions.

The discovery of ribozymes [1,2], which are RNAs that can catalyze chemical or biological reactions, in the early 1980s was the first hint that DNA might also be

Table 1 Different types of reactions catalyzed by DNAzymes.

Reaction type	Metal cofactor	Refs
RNA cleavage	Pb^{2+}	[3–10]
	Mg^{2+}	
	Zn^{2+}	
	none	
	Ca^{2+}	
	Mn^{2+} or Mg^{2+}	
	Mn^{2+} or Mg^{2+}	
	UO_2^{2+}	
DNA cleavage (oxidative)	Cu^{2+}	[11–13]
DNA cleavage (hydrolytic)	Zn^{2+} or Mn^{2+}	[14–16]
Phosphoramidate bond cleavage	Mg^{2+}	[17]
DNA ligation	Cu^{2+}, Zn^{2+} or Mn^{2+}	[18,19]
RNA ligation (3′-5′)	Zn^{2+} or Mg^{2+}	[20,21]
RNA ligation (branch formation)	Mn^{2+} or Mg^{2+}	[22–25]
RNA ligation (lariat formation)	Mn^{2+}	[26,27]
Nucleopeptide linkage formation	Mn^{2+} or Mg^{2+}	[28]
DNA phosphorylation	Mn^{2+}	[29]
DNA capping	Mg^{2+}, Cu^{2+}	[30]
DNA depurination (IO_4^--dependent)	none	[31]
DNA depurination	Ca^{2+}	[32]
Diels-Alder reaction	Ca^{2+}	[33]
Porphyrin metallation	Cu^{2+} or Zn^{2+}	[34,35]

capable of catalysis, because of the structural similarity between DNA and RNA. Such reasoning was not unfounded: in 1994, Ronald Breaker and Gerald Joyce isolated the first deoxyribozyme (DNAzyme) via *in vitro* selection [3]. This DNAzyme can catalyze a phosphodiester bond cleavage in the presence of Pb^{2+} and had a rate enhancement of 10^5 over the uncatalyzed reaction. After this initial discovery, many more DNAzymes have been successfully isolated which are able to catalyze various types of reactions. Table 1 lists representative DNAzymes that have been obtained, including DNAzymes that catalyze cleavage of RNA [3–10], DNA [11–16] or the phosphoramidate bond [17], the ligation of DNA [18,19] or RNA [20,21], the formation of an RNA branch [22–25], an RNA lariat [26,27], or a nucleopeptide bond [28], phosphorylation [29], adenylation [30], and depurination [31,32] of DNA, the Diels-Alder reaction [33], and porphyrin metallation [34,35]. One of the RNA-cleaving DNAzymes is capable of catalyzing a phosphodiester transfer reaction with a $k_{cat}/K_m \approx 10^9\ M^{-1}\ min^{-1}$ that rivals that of protein enzymes [4].

Interestingly, most DNAzymes carry out their catalysis with the aid of metal cofactors and some are very selective in this respect. For example, the first reported DNAzyme is about 400,000-fold selective for Pb^{2+} [3,36] over other competing metal ions and the UO_2^{2+}-dependent DNAzyme (39E) is >1 million-fold selective over other competing metal ions [10,37]. This kind of metal selectivity can be found in many other DNAzymes. Because of their generally high metal ion selectivity, DNAzymes have been converted into fluorometric [10,36,38–46], colorimetric [47–53], and electrochemical [54,55] sensors for metal ions. In addition, they have also been used to

detect and degrade specific RNA sequences because of the intrinsic sequence requirement for the DNAzyme activity [56–61].

Even though DNAzymes have proved their usefulness in many applications, the detailed structure and reaction mechanisms of the DNAzyme catalysis are still largely unclear. A large number of biochemical and biophysical studies have already been carried out for several DNAzymes, but the absence of any high-resolution, three-dimensional structure for the active conformations of DNAzymes is currently a major obstacle for understanding them [62,63]. In the meantime, biochemical and biophysical studies have offered insights into the conserved sequences and structural features responsible for DNAzymes' selective binding of metal ions and efficient catalysis.

In this chapter, we will first introduce *in vitro* selection (a method for isolating DNAzymes), then present the results of detailed biochemical and biophysical studies on RNA-cleaving DNAzymes. These studies have shed some light on how metal ions interact with DNAzymes. Finally, we will discuss the biosensing applications of DNAzymes.

2 *In vitro* Selection of DNAzymes

2.1 In vitro Selection

Although not yet found in nature, DNAzymes have been isolated via the combinatorial method of *in vitro* selection. This method was first developed in the 1990s to isolate ribozymes and RNA aptamers, single-stranded oligonucleotides with high affinities for different target molecules [64–66]. In 1994, Ronald Breaker and Gerald Joyce used this strategy to isolate the first DNA catalyst [3]. The first DNAzyme used Pb^{2+} as a cofactor to catalyze the cleavage of a phosphodiester bond.

In vitro selection starts with a "random pool" containing typically $10^{14–15}$ different DNA sequences. The pool is designed by flanking a random sequence with two constant regions that are primer binding sites (Figure 1). The length of the sequence generally varies from 40 to 80 nucleotides. After the "random pool" is then synthesized, it is incubated with the substrate to carry out the desired reaction in the presence of a cofactor. The active DNA sequences are partitioned and collected. The active sequences can be separated from the inactive ones by various methods, such as polyacrylamide gel electrophoresis (PAGE) or affinity resin. Polyacrylamide gel electrophoresis separates the reaction products according to their size-dependent mobility on a polymer matrix. Affinity separation normally employs biotinylated DNA and a streptavidin resin. After the separation step, polymerase chain reaction (PCR) is used to amplify the desired DNA sequences. Since *in vitro* selection normally only utilizes a single-stranded DNA (ssDNA), such ssDNA is then generated from the PCR products and they are incubated under the desired condition with the substrate to start the next round of selection. After iterative rounds of selection, separation, and amplification, the large initial pool of random sequences can be reduced into a small population of sequences that are enriched with active DNAzymes. Typically, it takes 5–15 rounds

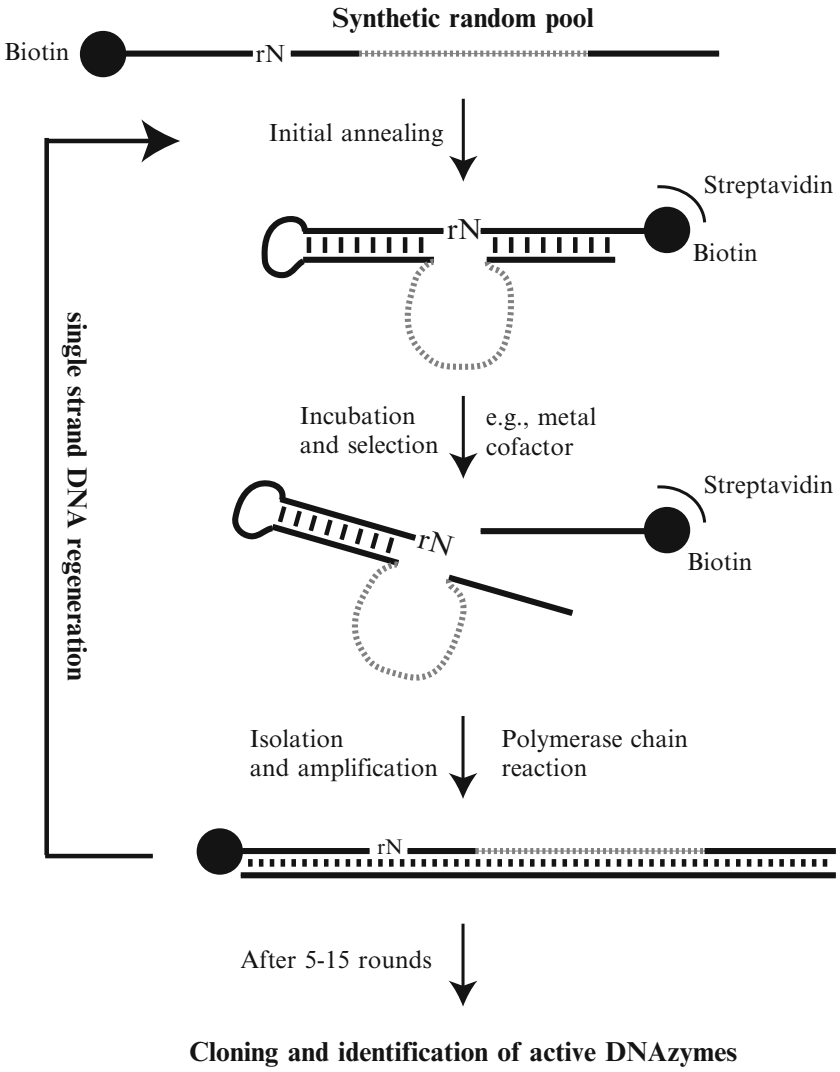

Figure 1 The schematic view of an *in vitro* selection process. rN denotes a ribonucleotide (as the cleavage site). Grey dotted line denotes the random region.

of selection to obtain an active DNAzyme. At this point, the population is cloned and sequenced. The resulting sequences are grouped into different families based on sequence similarity and each family is tested for activity. The DNAzyme selection is an application of the idea of "survival of the fittest", allowing researchers to find new DNAzymes with desirable activities in the presence of intended targets.

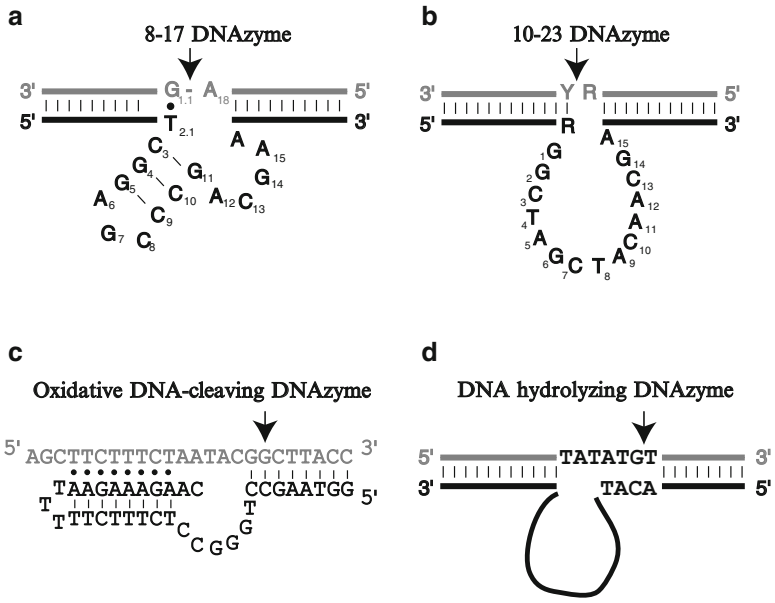

Figure 2 The predicted secondary structures for various RNA- and DNA-cleaving DNAzymes. Enzyme strands are in black and substrates are in grey. Black arrows indicate the cleavage site. Black lines between the enzyme and substrate strand indicate Watson-Crick base pairing. (**a**) The 8-17 DNAzyme; black dot indicates a wobble base pair. (**b**) The 10-23 DNAzyme, Y = pyrimidine, R = purine. (**c**) Ascorbate-independent DNA-cleaving DNAzyme, black dots indicate formation of triple helix; oxidative cleavage occurs on the sugar ring. (**d**) DNA-hydrolyzing DNAzyme.

2.2 Examples of Selected DNAzymes

Many DNAzymes have been isolated by *in vitro* selection. While most of the DNAzymes selected to date involve either cleaving or ligating the phosphodiester bond, DNAzymes with other functionalities have also been isolated, such as catalyzing porphyrin metallation and the Diels-Alder reaction.

2.2.1 RNA-Cleaving DNAzymes

The RNA-cleaving DNAzyme is the most frequently isolated and studied DNAzyme. They catalyze the phosphodiester bond cleavage of their RNA substrate. The 10-23 and 8-17 DNAzymes, first reported by Santoro and Joyce in 1997 [4], are the best-studied and most widely used RNA-cleaving DNAzymes (Figure 2a and 2b). They are named by the round and clone number in their respective selections. The computer algorithm mfold [67] has predicted that both DNAzymes have small catalytic cores of only 13 to 15 nucleotides. The 10-23 catalytic core is composed of an unstructured loop while the 8-17 catalytic core is composed of a three-base-pair stem, an

AGC trinucleotide loop, and an ACGA(A) loop. The cleavage site of 10-23 is a phosphodiester bond at the 3′-end of a single nucleotide flanked by two completely complementary substrate binding arms. The 8-17 cleavage site is similar to that of the 10-23 DNAzyme, but has an unpaired nucleotide with a G•T wobble pair immediately downstream from it. The initial selection of the 8-17 DNAzyme is only reported to cleave a 5′-AG-3′ junction, while the 10-23 DNAzyme is capable of cleaving any purine-pyrimidine (5′-RY-3′) junction [4]. Later biochemical characterizations indicated that both DNAzymes carry out the catalysis in a similar manner: metal assisted deprotonation of the 2′-hydroxyl, and the resulting oxyanion attacks the phosphate group nearby leading to cleavage [5,56,68–71]. This strategy is also used by naturally occurring ribozymes and endonucleases [72,73].

One surprising aspect of the 8-17 DNAzyme is that this DNAzyme has been isolated numerous times by different groups under very different conditions [5,7,9,70,74,75]. Several later selections were also carried out and isolated many more 8-17 variants. All these studies suggest that the 8-17 DNAzyme is a small, efficient sequence that occurs very frequently during *in vitro* selections. The large number of 8-17 variants aids later biochemical studies substantially [76].

The 10-23 DNAzyme has been widely used as a therapeutic agent for suppressing RNA levels in various systems [56,57,60] and for degrading viral RNA [58,59,61]. The 8-17 DNAzyme has numerous applications in nucleic acid detection [77,78], metal ion sensing [79–81] and DNA computing [82–87].

2.2.2 DNA-Cleaving DNAzymes

Besides catalyzing RNA cleavage, DNAzymes can also catalyze DNA cleavage via different types of mechanisms [11–16]. Because DNA is intrinsically more stable than RNA, DNAzymes that are capable of catalyzing DNA cleavage demand a higher degree of complexity than their RNA-cleaving siblings. The first DNA-cleaving DNAzymes were isolated in 1996 by Carmi, Schultz, and Breaker [11]. Both of the DNAzyme classes identified in this experiment catalyze DNA cleavage via an oxidative mechanism; what distinguishes them is that they have different requirements for cofactors: the Class I catalyst requires both Cu^{2+} and ascorbate while the Class II catalyst requires only Cu^{2+}. However, these DNAzymes are not site-selective and their oxidative cleavage mechanism limits their application to *ex vivo* purposes [11–13]. Other DNA-cleaving DNAzymes were isolated in 2009 by Chandra, Sachdeva, and Silverman [14]. Unlike the Cu^{2+}/ascorbate-dependent DNAzymes, these new DNAzymes are capable of cleaving DNA by a hydrolytic mechanism using Zn^{2+} and Mn^{2+} as cofactors [14–16].

2.2.3 DNAzymes that Catalyze Ligation Reactions

The reverse reaction of RNA or DNA cleavage, RNA or DNA ligation, can also be catalyzed by DNAzymes. The first RNA-ligating DNAzyme was isolated in 2003

by Flynn-Charlebois et al. [88,89]. This DNAzyme is capable of ligating a RNA fragment with a 2′,3′-cyclic phosphate to the 5′-hydroxyl of a second RNA fragment. The phosphodiester bond formed by this DNAzyme is a 2′-3′ linkage, unlike the naturally occurring 3′-5′ linkage in DNA [88,89]. On the other hand, an RNA-ligating DNAzyme that formed a 3′-5′ linkage was isolated in 2005. A 5′-triphosphate RNA and a DNAzyme that cleaves the 3′-5′ linkage were introduced into the selection process to favor the formation of the natural linkage [21,90]. Detailed information on the RNA-ligating DNAzymes can be found elsewhere [56,91]. Besides RNA ligation, DNA-ligating DNAzymes have also been reported [18,19].

2.2.4 Other DNAzymes

Other types of reactions that DNAzyme catalyze are listed in Table 1. While most DNAzymes selected so far catalyze reactions that modify a nucleic acid substrate, two DNAzymes in particular catalyze reactions on non-nucleotide substrates: the PS2.M DNAzyme and the DAB22 DNAzyme [33,34].

The PS2.M DNAzyme was originally isolated as a DNA sequence that specifically binds to *N*-methylmesoporphyrin (NMM), a transition-state analogue of a porphyrin metallation reaction [34,35,92,93]. Later studies indicate that hemin [Fe(III)-protoporphyrin IX], an inhibitor of porphyrin metallation, can also bind to the PS2.M DNAzyme, and the DNAzyme/hemin complex can catalyze the peroxidation of 2,2′-azino-bis(3-ethylbenzthiazoline-6-sulfonic acid) (ABTS) or luminol [35,93,94]. The rate of the DNAzyme catalyzed peroxidation is approximately 250 fold higher than the background rate measured in the presence of a control oligo. Instead of forming a helical structure, the 18-nucleotide PS2.M DNAzyme is proposed to have a G-quadruplex structure due to its high guanine content. This G-quadruplex structure of the PS2.M DNAzyme is also crucial for its metallation and peroxidase activity [93–96].

The DAB22 DNAzyme was isolated to catalyze a Diels-Alder reaction. It catalyzes the carbon-carbon bond formation between an anthracene and a maleimide with a rate of 0.7 M^{-1} s^{-1} [33]. This rate is comparable to the ribozyme counterpart which carries out the same reaction [97].

3 Biochemical Mass Spectrometric Studies of DNAzymes

Among the various types of DNAzymes, the RNA-cleaving DNAzymes have been best characterized because of their wide practical applications. These DNAzymes have been studied biochemically via activity assays, mass spectrometry, and UV-induced cross-linking assays. These biochemical assays have provided information about the conserved motifs and catalytic mechanisms of these DNAzymes.

Table 2 Activity of the 8-17 and 10-23 DNAzymes in the presence of different metal ions.

	Metal cofactor	k_{obs}, min^{-1}	k_{cat}/K_m	pK_a	Refs
10-23 DNAzyme	50 mM Mg^{2+}	3.4	4.5×10^9	11.4	[4,71,98]
	25 mM Mn^{2+}	1.19	7.0×10^7	10.6	
	25 mM Ca^{2+}	0.863	1.4×10^7	12.9	
	25 mM Mg^{2+}	0.961	2.2×10^7	11.4	
	25 mM Ba^{2+}	0.101	0.26×10^7	13.5	
	10 mM Mn^{2+}	>4	n.r.	10.6	
	10 mM Mg^{2+}	0.28	n.r.	11.4	
	10 mM Ca^{2+}	0.12	n.r.	12.9	
	10 mM Sr^{2+}	0.026	n.r.	13.2	
	10 mM Ba^{2+}	0.015	n.r.	13.5	
8-17 DNAzyme	2 mM Mg^{2+}	≈0.01	n.r.	11.4	[4,68,70]
	0.2 mM Pb^{2+}	0.47	n.r.	7.8	
	5 mM Zn^{2+}	12	n.r.	8.96	
	3 mM Mn^{2+}	≈0.1	n.r.	10.6	
	3 mM Mg^{2+}	≈0.002	n.r.	11.4	
	3 mM Ca^{2+}	≈0.02	n.r	12.9	
17E DNAzyme (8-17 variant)	0.1 mM Pb^{2+}	5.75	n.r.	7.8	
	10 mM Zn^{2+}	1.35	n.r.	8.96	[68]
	10 mM Mn^{2+}	0.24	n.r.	10.6	
	10 mM Mg^{2+}	0.017	n.r.	11.4	
	10 mM Ca^{2+}	0.015	n.r.	12.9	
Mg5 DNAzyme (8-17 variant)	0.2 mM Pb^{2+}	2.1	n.r.	7.8	
	5 mM Zn^{2+}	0.74	n.r.	8.96	[68,70]
	3 mM Mn^{2+}	> 3	n.r.	10.6	
	3 mM Mg^{2+}	0.06	n.r.	11.4	
	3 mM Ca^{2+}	1	n.r.	12.9	

n.r. = not reported

3.1 Activity Assays

When these DNAzymes cleave their RNA-containing substrates, they generate products with different lengths. Thus, their activity can be easily monitored by PAGE. Vital information on these DNAzymes can be obtained by combining the activity assays with mutational studies.

The 10-23 and 8-17 DNAzymes have been studied most extensively by these methods [4,68–70,98]. Basic biochemical parameters and their metal-dependent changes have been extracted from these studies and are shown in Table 2 (different variants of the 8-17 DNAzymes have also been shown for comparison). Both 10-23 and 8-17 DNAzymes can catalyze reactions very efficiently: their catalytic rates approach 10 min^{-1}, which is very close to that of naturally existing ribozymes [4]. Studies on the metal dependence of the 8-17 DNAzyme and its variants are much more extensive than that of the 10-23 DNAzyme. A study by the Lu group and

others in 2003 demonstrated that the 17E, as well as other 8-17 DNAzymes, has a higher reaction rate in the presence of Pb^{2+} [68]. Interestingly, although both the 10-23 and 8-17 DNAzymes were selected in the presence of Mg^{2+}, Mg^{2+} is not the metal cofactor that can induce the highest catalytic activity. Instead, Mn^{2+} promotes the highest activity for the 10-23 DNAzyme and Pb^{2+} has the same effect for the 8-17 DNAzyme [68,71,98].

In addition to the rate constants and metal dependence, important information about the conserved sequences required for the activities of these enzymes was obtained through mutational studies [98–100]. In these studies, nucleotides in different positions in the DNAzyme were replaced with natural or unnatural bases, revealing the importance of the nucleotide or functional group at particular positions (Figure 2a and 2b). A deletion study carried out in 2004 [100], agrees with the original hypothesis that the 10-23 core is almost intolerant to mutations: only C_7 and T_8 deletion remain highly active. A C_7/T_8 double deletion resulted in a 10-fold decrease in the catalytic rate in the presence of Mg^{2+} [4,101]. Interestingly, a four-nucleotide deletion ($A_5G_6C_7T_8$) from the 10-23 DNAzyme still resulted in an active enzyme and the resulting DNAzyme was highly selective for Ca^{2+} [98]. Systematic mutagenesis of the 10-23 DNAzyme's catalytic core revealed that the nucleotides closer to the borders (e.g., G_1, G_2, T_4, G_6, and G_{14}) are the least tolerant to mutation, while nucleotides in the center are much more tolerant [99]. Only a few of the mutations in the region from positions 7-12 reduce the activity of the DNAzyme, which is not consistent with the original report in 1997 [4]. In the same study, the authors have also tried to replace certain nucleobases with inosine and other nucleobase analogs such as 2-aminopurine and purine. The nucleotide analog substitutions indicate that the functional groups on certain bases are crucial for the 10-23 DNAzyme's activity, such as the 2-amino and the 6-keto groups on G_{14}, as well as the exocyclic amino group on A_5.

Similar investigations on the 8-17 DNAzyme and its variants [68,102] suggested a sequence requirement that is very close to the original proposal [4], including the importance of a G•T wobble pair next to the cleavage site, a AGC loop, a 3-base pair stem and a single-stranded region with the sequence WCGA(A) (W = A or T). An unnatural nucleotide substitution study has also been performed on the 8-17 catalytic core, stressing the critical role of N7 on A_6, O6 on G_7, and N2 on G_{14} [102]. Although the 8-17 DNAzyme was initially reported to cleave only a 5′-AG-3′ junction, later studies on other 8-17 variants demonstrated their capability to cleave all sixteen possible dinucleotide junctions with different rates [5,9,68,75]. Mass spectrometric analysis of the substrate cleaved by the 8-17 DNAzyme suggested that different products were formed in the presence of different metal ions [5,68]. When the cleavage reaction is catalyzed by Zn^{2+} or Mg^{2+}, the formation of 2′,3′-cyclic phosphate (at the 3′-terminus) was observed by MALDI-TOF mass spectrometry; when the reaction was catalyzed by Pb^{2+}, 3′ (or 2′) monophosphate formation is observed at the 3′-terminus [68].

In a recent mutational study, an abasic nucleotide or C3 acrylic spacer was substituted for the key residues within the catalytic core of the 8-17 and 10-23 DNAzymes [103]. Besides reconfirming that certain nucleotides are absolutely

required for the activities of these DNAzymes, the authors proposed that many other nucleotides within the catalytic core perform a chaperone-like function and they are only important for the optimal activity of the DNAzyme. Four nucleotides are absolutely required for both the 8-17 and 10-23 DNAzymes and coincidentally, the positions and neighboring nucleotides of these four nucleotides are very similar.

3.2 Cross-linking Studies

The activity assays have provided vital information on the sequence and metal cofactor requirements of the DNAzymes, but very little information about the structure of the DNAzymes. Several cross-linking studies carried out by the Sen group have provided some insight into the spatial arrangement of the DNAzyme [104–106]. In these studies, halo- and thiosubstituted nucleotides were used to replace some of the nucleotides in the catalytic core of the 8-17 DNAzyme. Upon irradiation with UV light, these halo- and thiosubstituted nucleotides formed cross-linked adducts with nucleotides that are contacting. These adducts can be treated with piperidine, which causes the linked nucleotides to undergo deglycosylation and β-elimination at the 3′ phosphate, resulting in strand cleavage [107]. The site of the crosslink can then be identified via PAGE [104].

The cross-linking study on the 8-17 DNAzyme in the presence of Mg^{2+} revealed strong interaction between nucleotides in the $A_6G_7C_8$ loop, and particularly $C_{13}G_{14}$ with $T_{2.1}$ in the wobble pair (Figure 2a). This result is in close agreement with previous mutational studies [68,102], stressing the importance of these nucleotides for the catalytic activity of the 8-17 DNAzyme. The authors provided a more interactive picture on the active site of the 8-17 DNAzyme based on available data: the AGC loop and the WCGAA region bend toward the cleavage site and the G•T wobble pair, forming close contacts between $T_{2.1}$, A_6, G_7, C_{13} and G_{14} [104]. A follow-up study addressing the cross-links formed in the presence of Pb^{2+} showed only local contacts. No global rearrangements, e.g., contacts between the AGC loop and $T_{2.1}$, were observed [105]. This Pb^{2+}-dependent study, together with the mass spectrometric analysis of the cleavage products [68] and FRET studies [108,109], suggest that Pb^{2+} is a unique metal cofactor for the 8-17 DNAzyme. A stereo-chemical study of the active site residues of the 8-17 DNAzyme have also been reported using an iodine-mediated cross-link approach. The study revealed that C_{13} occupies an asymmetrical position which is critical for catalysis [106].

Another study by Leung and Sen used an electron hole flow pattern, and suggested that C_{13} and G_{14} in the single-stranded loop region are highly solvent exposed. This observation agrees with what was previously known: that these two nucleotides are critical for catalysis. G_7, in contrast, is not solvent-exposed, but is similar to a guanine within a double helix. This observation suggests that G_7 helps organizing the active site [110]. G_7's lesser extent of solvent exposure seems to be in agreement with a previous study that indicated that G_7 is sensitive to steric hindrance [102].

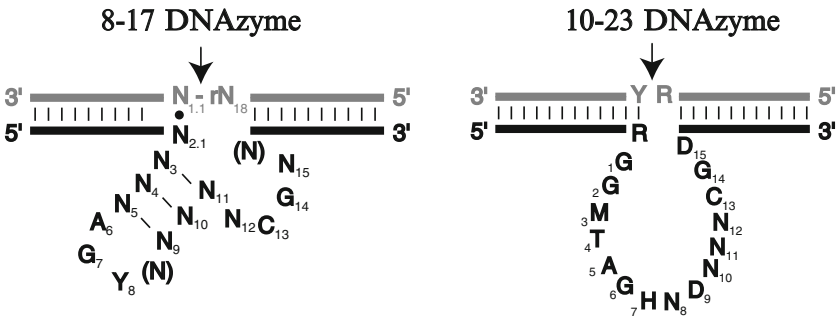

Figure 3 The conserved nucleotides in the 8-17 and 10-23 DNAzymes. N = A, T, C or G; r = ribonucleotide; Y = T or C; R = A or G; M = A or C; H = A, C or T; D = A, G or T; the arrow denotes the cleavage site.

3.3 Conserved Sequences and Motifs of DNAzymes

Among all the DNAzymes, the conserved sequence for the 8-17 DNAzyme is the most extensively studied. The members of this sequence family isolated from *in vitro* selections by several groups [4,5,7,70,111] provide a good starting point for analyzing its sequence conservation. The first published study of this DNAzyme suggested that its conserved sequence included the G•T wobble base pair, a 3-base pair stem, an AGC trinucleotide loop, and a single-stranded region with the sequence WCGR(A) (W = A or T; R = A or G) [68,102]. Later studies have shown that the conserved sequence of the 8-17 DNAzyme is smaller than previously thought, especially when the cleavage site is taken into account [9,75,112]. Based on these studies, only four nucleotides are strictly conserved: A_6, G_7 in the tri-nucleotide loop, and C_{13}, G_{14} in the single-stranded region (see Figure 3).

Although not as extensively studied as the 8-17 DNAzyme, the motif for the 10-23 DNAzyme has also been defined (Figure 3) [4,100,101,103]. Other DNAzyme motifs have been identified through *in vitro* selection as well, but the sequence conservation of these DNAzyme motifs has not been studied yet in detail.

3.4 Reaction Mechanisms

Based on the biochemical studies carried out to date, the reaction mechanism of most RNA-cleaving DNAzymes is believed to be consistent with metal-assisted general acid-base catalysis. However, without the three-dimensional structure of any active DNAzyme, a detailed mechanism is still out-of-reach. In the case of the 8-17 DNAzyme, cleavage product analysis shows that (with the exception of the Pb^{2+}-catalyzed reaction) the products contain a 2′,3′-cyclic phosphate at the 3′-terminus and a 5′-hydroxyl at the 5′-terminus [5,68]. These cleavage products indicate

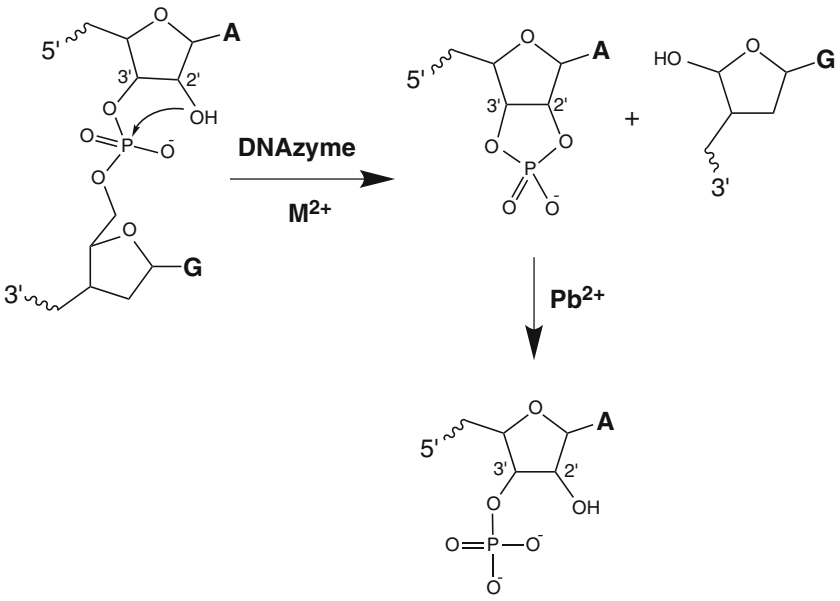

Figure 4 The proposed mechanism for the 8-17 catalysis based on biochemical studies on the 8-17 DNAzyme. The hydrolysis of the cyclic phosphate to monophosphate only occurs in the presence of Pb^{2+}.

a nucleophilic attack from the 2′-hydroxyl on the scissile phosphodiester bond. The attack results in a 5-coordinated phosphate intermediate and the cleavage of the P-O bond leading to the formation of the products. In the presence of Pb^{2+}, the cyclic phosphate is further hydrolyzed to a monophosphate (Figure 4) [68]. This second step hydrolysis by Pb^{2+} is observed in leadzyme (ribozyme) and protein ribonucleases. From other studies, the rate of 8-17 catalyzed reactions plotted versus pH on a logarithmic scale is linear with a slope of one [5,68,113,114]. This observation suggests a single deprotonation event is the rate-limiting step, and this can be assigned to the nucleophilic attack of the 2′-hydroxyl.

A linear relationship between the rates of the reaction and the pK_a values of the active metal cofactor hydrates has also been observed. This observation supports the idea that the deprotonation of the 2′-hydroxyl is assisted by the corresponding metal cofactors [72,73]. Direct metal coordination is probably required for the 8-17 DNAzyme catalysis, since the cobalt complex $[Co(NH_3)_6]^{3+}$ (a structural analogue of hexahydrate Mg^{2+}, but incapable of coordinating to the ribose, phosphate and water) does not support the activity of the DNAzyme [115]. That no significant activity can be observed for the DNAzyme in the presence of high concentration of monovalent ions, may also suggest that the metal cofactor plays a direct role in catalysis [116]; in addition, metal cofactors can also assist the folding of this DNAzyme. The 10-23 DNAzyme also employs a very similar mechanism, except for the hydrolysis of the cyclic phosphate to the monophosphate [69,71,103,117].

4 Biophysical Studies of DNAzymes

To date, no three-dimensional X-ray or NMR structure of a DNAzyme in an active conformation has been published. The only crystal structure available is a 10-23 DNAzyme that resembles a 2:2 enzyme:substrate complex in a four-way junction. This stoichiometry and conformation do not reflect the active form of the 10-23 DNAzyme. As work to obtain the three-dimensional structure of an active DNAzyme continues, the structure and folding of DNAzymes are being studied by various spectroscopic methods, such as Förster resonance energy transfer (FRET), circular dichroism (CD), Tb^{3+} luminescence, and NMR.

4.1 FRET and Single Molecule FRET Studies

FRET is a widely accepted technique for studying the structural dynamics of biomolecules in solution [118–121]. Various types of macromolecule structures, such as double-stranded DNA, three- and four-way DNA junctions, hammerhead and hairpin ribozymes; as well as dynamic process, such as DNA/RNA folding, ribozyme catalysis, DNA/protein interactions, have been studied by FRET [122–134]. In a FRET experiment, the molecule is labelled with donor and acceptor fluorophores that exhibit spectral overlap between donor emission and acceptor excitation. Upon the excitation of the donor, fluorescent energy can transfer to the acceptor depending on the distance between the two. The efficiency of the energy transfer is highly sensitive to inter-fluorophore distance. From the change of the FRET efficiency, the global conformation change can be deduced [135]. Although FRET studies are normally carried out with dual fluorophores, multi-fluorophore FRET has also been applied in protein studies [136-138].

The first FRET study on the 8-17 DNAzyme involved a tri-fluorophore labelled DNAzyme [135]. The 8-17 variant used in the study, 17E, was an inactive construct where the ribose at the cleavage site has been replaced with a deoxyribose. The three arms of the DNAzyme are labelled with three fluorophores: 6-carboxyfluorescein (FAM), Cy5, and 6-carboxytetramethylrhodamine (TMR) (as shown in Figure 5a). The FRET efficiency changes between FAM-TMR, FAM-Cy5, and TMR-Cy5 were monitored and the global conformation changes of the DNAzyme were monitored in the presence of Zn^{2+}. The result indicates that the 17E DNAzyme undergoes a two-step folding process in the presence of Zn^{2+}: at low Zn^{2+} concentrations, the FAM-labelled arm folds towards the Cy5-labelled arm with a K_d of 19 μM; at higher concentration of Zn^{2+} (K_d = 260 μM), the TMR-labelled arm folds towards the other two arms, forming a more compact structure.

Another tri-fluorophore labelled FRET study emphasizing the folding of the 8-17 DNAzyme with different cleavage junctions has also been carried out [139]. The study also revealed that the DNAzyme undergoes two-step folding in the presence of Mn^{2+}, where the first folding step occurs at 1–10 mM Mn^{2+} and is

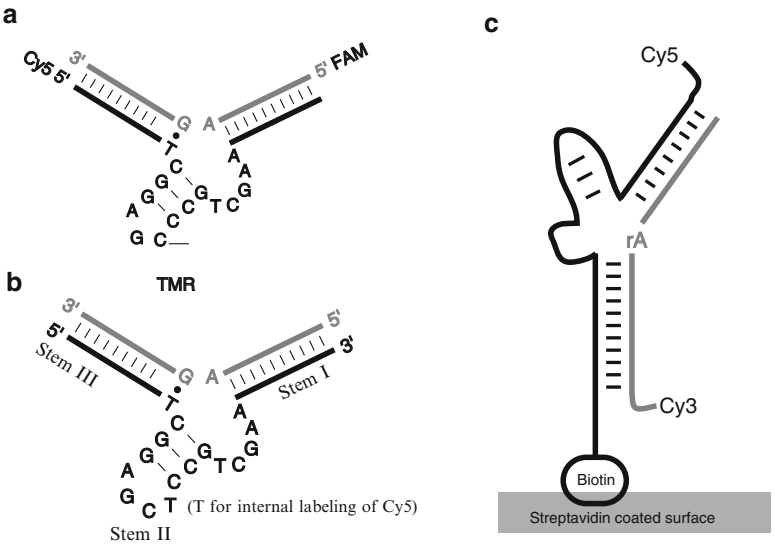

Figure 5 The 8-17 constructs used in various FRET studies. (**a**). The construct used for the tri-color FRET. (**b**). The construct for the bulk FRET study. Pairs of Cy5/Cy3 are separately labelled on Stem I/II, Stem II/III and Stem I/III. A thymine on Stem II is used for internal Cy5 labelling. FRET efficiencies between different stems were measured. (**c**). The construct for a smFRET study contained a riboA at the cleavage site. The Cy5 and Cy3 labelled DNAzyme:substrate complex is attached on the glass slide via a biotin-streptavidin interaction. The time-dependent FRET efficiency was monitored in the presence of different divalent metal ions.

independent of the cleavage junction, and the second folding step occurs at 20–200 mM Mn^{2+} and is dependent on the cleavage junction. The 8-17 DNAzymes with purine-purine junctions folded at lower Mn^{2+} concentration than the ones with pyrimidine-pyrimidine junctions [139].

In 2007, two more FRET studies provided a more complete view on the metal-dependent global folding and folding dynamics of the 8-17 DNAzyme (Figure 5b) [108,109]. Global folding of the DNAzyme was observed for both Zn^{2+} and Mg^{2+} and lower concentration of Zn^{2+} than Mg^{2+} is required for the process. This observation is consistent with the fact that the 8-17 DNAzyme was active at lower concentrations of Zn^{2+}. However, no conformational change is observed in the presence of Pb^{2+}, the metal ion cofactor that supports the highest level of activity [108]. The second single molecule FRET (smFRET) study addressed the problem that the 8-17 DNAzyme construct used in the ensemble FRET was inactive (Figure 5c). The reaction catalyzed by the 8-17 DNAzyme is followed in real-time in the smFRET study. Fluorescence time trace for each individual molecule was recorded and the FRET efficiency was monitored. Changes in the FRET efficiency corresponded to an individual state in the dynamic process. In the presence of Zn^{2+} and Mg^{2+}, a folded state is observed before cleavage. In contrast, in the presence of Pb^{2+}, cleavage is observed

without a folding step. These results reveal that the 8-17 DNAzyme uses an "induced fit" catalytic mechanism in the presence of Zn^{2+} and Mg^{2+} while using a "lock-and-key" mechanism in the presence of Pb^{2+}. These results may help to explain why Pb^{2+} can support the highest rate of reaction [109].

A comprehensive investigation on the folding and activity of the 8-17 DNAzyme in the presence of monovalent ions has been conducted by Mazumdar et al. [116]. Folding is observed by ensemble FRET for all monovalent ions examined in the study at high concentrations (Li^+, Na^+, NH_4^+, Rb^+, and Cs^+), while only Li^+, Na^+, and NH_4^+ confer activity.

A newly developed, three-color, alternating-laser excitation FRET method has been reported for studying the 8-17 DNAzyme with similar results. This new method may provide more detailed insights into the folding and reaction dynamics of DNAzymes in general [140,141].

4.2 NMR Studies

Although NMR spectroscopy can provide vital information on the specific interactions between the nucleotides in the DNAzyme, only a limited number of NMR studies have been carried out with DNAzymes. The ^1H NMR spectra for the lead-dependent DNAzyme selected in 1994 was first obtained. No significant chemical shift was observed when 0–19 mM Mg^{2+} was titrated into the DNAzyme in solution. Unfortunately, no Pb^{2+} titration was performed, since Pb^{2+} is the active metal cofactor. NMR spectroscopy has also been attempted on the 10-23 DNAzyme, but only the base pairing features between the substrate binding arms can be resolved; no information on the catalytic core was provided [101]. Further NMR analysis on DNAzymes could assist the understanding of the specific interactions, such as the DNA/DNA and DNA/metal interactions, and the catalytic mechanism [142].

4.3 Other Spectroscopic Studies

Lanthanide ions (Lu^{3+}, Tb^{3+}, Eu^{3+}) have often been used as spectroscopic probes for nucleic acids, since they show sensitized luminescence by energy transfer from the nucleic acids [143–149]. They are used in many ribozyme studies to probe the metal binding sites by competing with other cations. Luminescence lifetime measurements can be used to determine the number of water molecules coordinated to the lanthanide ions.

Tb^{3+} luminescence spectroscopy was recently used to study the metal binding in the 8-17 DNAzyme [150]. Tb^{3+} can competitively and reversibly inhibit the Zn^{2+}- and Pb^{2+}-dependent enzyme activity. This property of Tb^{3+} allowed a further study of the metal ion binding of the DNAzyme. Luminescence lifetime measurements indicated that 6–7 water molecules were coordinated to Tb^{3+}. Since nine water

molecules are normally coordinated to Tb^{3+}, 2–3 water molecules were replaced by functional groups in the DNAzyme. A competition study indicated that Tb^{3+} competes differently for the Pb^{2+} binding site from binding sites of other metal ions such as Zn^{2+}, Mn^{2+}, Co^{2+}, Ca^{2+}, and Mg^{2+}. This study provides additional evidence for a unique interaction between Pb^{2+} and the 8-17 DNAzyme, which has been indicated by all previous biochemical and biophysical studies.

In contrast to the inhibitory effect observed for the 8-17 DNAzyme, lanthanide ions are able to support the RNA-cleaving activity of the lead-dependent DNAzyme selected in 1994 [151]. However, the mode of catalysis appears to be different from that of the lead driven catalysis. No pH-dependent activity was observed for any of the lanthanide ions tested, while a pH dependent activity is generally observed for Pb^{2+}. The luminescence measurements indicate that the substrate alone is sufficient for binding the Tb^{3+} ion. Absence of the 2′-hydroxyl group on the substrate eliminated Tb^{3+} binding.

CD spectroscopy has also been used to study structural changes of the 8-17 DNAzyme [116]. The transition between the right-handed B-form DNA to the left-handed Z-form DNA can be monitored by CD spectroscopy. Formation of Z-DNA, as indicated by a negative peak at 294 nm, can be induced in the presence of molar concentrations of monovalent ions, such as Li^+, Na^+, Rb^+, Cs^+ or NH_4^+ for DNA sequences with alternating GC bases [152–157]. More importantly, the Z-DNA formation is also observed in the presence of micromolar concentrations of Zn^{2+} and millimolar concentrations of Mg^{2+}. The Z-DNA formation is attributed to the three-base-pair stem in the catalytic core, since the mutation of the middle GC to AT eliminates the Z-DNA formation. No Z-DNA formation is observed in the presence of Pb^{2+}. The CD study correlates very well with previous FRET studies showing that Zn^{2+} and Mg^{2+} have a different mode of interaction with the DNAzyme from Pb^{2+} [108,109].

4.4 Structural Features Learned from the Biophysical Studies

Without any high-resolution crystal or NMR structure of an active DNAzyme, the precise structure of the DNAzyme responsible for the catalytic activity is largely unclear. However, from the biochemical and biophysical studies, certain important structural features of DNAzymes, especially those of the 8-17 DNAzyme, can be deduced and are summaried below.

First, global folding of the 8-17 DNAzyme in the presence of Zn^{2+} and Mg^{2+} (as well as high concentrations of monovalent ions) can be observed and this folding is required for activity. Second, a local B-to-Z DNA transition occurs in the stem region inside the catalytic core. Third, the cross-linking study points out that several key nucleotides make contact in the catalytic core: the AGC trinucleotide loop folds back and contacts the dinucleotide cleavage junction; C_{13} and G_{14} are also in close contact with the cleavage junction. Fourth, the metal binding site appears to be in the WCGAA region as mutagenesis studies indicated. Last, Pb^{2+} is the exception to

all four points mentioned above as no global folding or B-to-Z DNA transition is observed in the presence of Pb^{2+}. In addition, limited nucleotide contacts are detected via the photo cross-linking study and the site of Pb^{2+} binding, as indicated from all the studies, is different from that of Zn^{2+} and Mg^{2+} binding.

Some of these structural features can be also observed for the 10-23 DNAzyme, such as the structural rearrangement to a more compact structure upon Mg^{2+} binding [158]. The nucleotide responsible for metal binding is also deduced [117]. However, these studies on the 10-23 or other DNAzymes are much less comprehensive in comparison with those of the 8-17 DNAzyme.

5 Biosensing Applications of DNAzymes

Heavy metal ion contamination can often pose significant hazards to the health of the general public and the environment. Developing analytical tools for their detection is an important way to monitor contamination. Currently, heavy metal ions are analyzed by various instrumental techniques, such as atomic absorption spectrometry, inductively coupled plasma mass spectroscopy, anodic stripping voltammetry, and X-ray fluorescence spectrometry. Although these instrumental techniques are very sensitive to heavy metals (often lower than ppb level) [159], they require advanced equipment, skilled operators, and pretreatment of samples, and therefore, on-site and real-time monitoring is difficult to achieve [160–162].

The rational design of small-molecule based chemical sensors for metal ions are challenging because it often involves try-and-error processes. The combinatorial search for metal ion sensors presents a new opportunity. Isolated from combinatorial *in vitro* selection experiments, DNAzymes often possess high metal selectivity, such as the 8-17, 39E, and the classic lead-dependent DNAzyme [3,5,10,68]. These RNA-cleaving DNAzymes are specific for a wide range of metal ions, have small catalytic domains, and have a fast reaction rate [163–167]. Combined with the high stability and the low cost of synthesis for DNA, DNAzymes represent good candidates for biosensing applications.

5.1 Fluorescence Sensors

Fluorescence-based sensors can provide high sensitivity with common benchtop or even portable fluorometers. Fluorophores and quenchers are normally covalently attached to DNA in fluorescence-based DNAzyme sensors. Recently, fluorescence sensors without chemically linked fluorophores have also been developed. These labelled free sensors without the chemically linked fluorophores have benefits due to their lower cost.

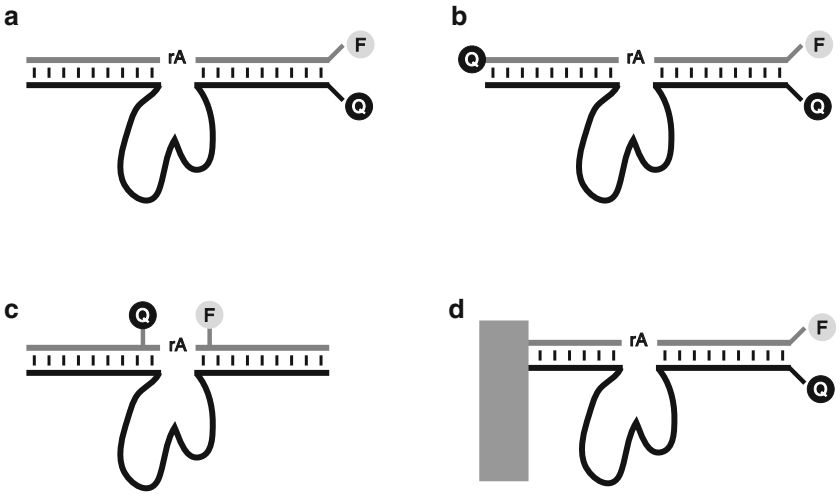

Figure 6 Designs for labeled fluorescence sensors. F denotes a fluorophore and Q denotes a quencher in general. rA denotes the cleavage site. Different fluorophores and quenchers could be used in different studies.

5.1.1 Labelled Fluorescence Sensors

The first fluorescence DNAzyme sensor was reported in 2000 by Li and Lu based on the 8-17 DNAzyme for the detection of Pb^{2+} (Figure 6a) [38]. In this sensor, the fluorophore 6-carboxytetramethylrhodamine (TAMRA) was covalently attached to the 5′-end of the substrate strand and a quencher (4-(4′-dimethylaminophenylazo)benzoic acid, or Dabcyl) was attached to the 3′-end of the enzyme strand. As a result, in the absence of Pb^{2+}, the enzyme and substrate were held together by Watson-Crick base-pairing because the melting temperature was above room temperature, resulting in a low fluorescence quenched state. In the presence of Pb^{2+}, the 8-17 DNAzyme catalyzed the cleavage of the substrate. The cleaved substrate was unstable at room temperature due to its lowered melting temperature with its complementary strand, and therefore it was released from the enzyme strand. The end result was that the fluorophore was separated from the quencher and an increase in the fluorescence could be detected with a fluorometer. By this design, the DNAzyme based biosensor is able to detect Pb^{2+} at concentrations as low as 10 nM, which is lower than 72 nM, the maximum contamination level for drinking water as defined by the U.S. EPA.

The sensor also has 80–1000 fold selectivity against other metal ions because of the intrinsic selectivity of the 8-17E DNAzyme [68]. One drawback of this design is the high background fluorescence even when the assay is carried out at 4°C. As a result, only a low fluorescence enhancement is observed (60%). In a new design, a second intramolecular quencher was introduced into the system and an over six-fold

increase in fluorescence was obtained at room temperature (Figure 6b) [39]. Because of the robust performance, many of the newer fluorescent sensors have been based on this dual-quencher design [10,36,40–42,168].

Some of these sensors possess extremely high sensitivity and selectivity, in some cases they can surpass many instrumental methods. For example, a fluorescent sensor based on the UO_2^{2+}-dependent 39E DNAzyme with incorporated asymmetric substrate binding arms and a dual-quencher can detect as low as 45 pM of UO_2^{2+} in solution, which is lower than the detection limit of ICP-MS for uranium (420 pM) [10]. The toxic level in water for uranium is 130 nM defined by the U.S. EPA. Besides its high sensitivity, this sensor also has an over 1-million fold selectivity against the next best competing ion Th(IV) and hundreds of millions fold selectivity over other metal ions [169]. The improved Pb^{2+} sensor based on the lead-dependent DNAzyme can also offer a 40,000-fold selectivity against other metal ions [36], which is a significant improvement over the 8-17 DNAzyme-based sensors.

Besides modifying the termini of the DNAzyme and the substrate, internal labelling of the fluorophore and quencher can also be used (Figure 6c). Both rational design and combinatorial selection methods have been used for such a sensor design. In the rational design study, different fluorophore and quencher pairs were placed on various positions across the cleavage site of the 8-17 DNAzyme. In general, higher fluorescence enhancement was obtained from the internally labelled fluorophore and quencher, with the strongest signal producing an 85-fold enhancement [170]. Combinatorial selection of metal sensors can be accomplished by introducing a fluorophore and a quencher into the *in vitro* selection of metal-dependent DNAzymes. This type of selection has been carried out by Li and coworkers and they have isolated DNAzymes with high fluorescent enhancements and high catalytic rates [171,172].

Replacing organic dyes with quantum dots (QDs) has become popular. Quantum dots have advantages over organic dyes in terms of their size-dependent emission, single wavelength excitation, higher quantum yield and higher photo stability [173,174]. Therefore, using QD can potentially give higher sensitivity and allow multiplex detection. Using QD-linked DNAzymes, Wu and coworkers demonstrated the simultaneous detection of Pb^{2+} and Cu^{2+} with very high sensitivity (0.2 nM for Pb^{2+} and 0.5 nM for Cu^{2+}). In this study, QDs with different emissions were attached to the substrates of the 8-17 DNAzyme and a Cu^{2+}-dependent DNAzyme; the substrate was also covalently attached to a quencher at the 3′-terminus. Both DNAzymes also had a quencher attached at the 5′-terminus. Before cleavage, the fluorescence of the QDs were quenched; after addition of metal ions, cleavage of the substrates released the quenchers and fluorescence enhancement could be observed when the QDs were excited with a single excitation wavelength [175]. Replacing the quencher with gold nanoparticles can also achieve a lower detection limit because of the better quenching by gold nanoparticles compared to organic dyes [176,177]. A recent study has demonstrated that use of a gold nanoparticle, a fluorophore dual-labelled substrate, and the 8-17 DNAzyme can achieve a detection limit as low as 5 nM [178].

5.1.2 Label-Free Fluorescence Sensors

Labelling the DNAzyme with fluorescent tags costs extra time and materials and they may potentially interfere with enzymatic activities. Therefore, fluorescence sensors without these external tags will have an advantage in these aspects. Recently, several label-free fluorescence sensors have been developed by various groups.

One of the methods for designing label-free sensors involved DNA intercalating dyes. The extrinsic fluorophore 2-amino-5,6,7-trimethyl-1,8-naphthyridine (ATMND) was demonstrated to be a general route to design label-free fluorescence sensors. In two different studies, an abasic site or vacant site was introduced into the double-stranded region of the 8-17 DNAzyme-substrate complex. The fluorophore ATMND can bind to the opposite nucleotide of the abasic or vacant site via hydrogen bonding and base stacking. When ATMND is bound, its fluorescence is quenched. Upon cleavage, the release of the substrate causes the release of ATMND into solution, resulting in a fluorescence enhancement. This design was applied to both the 8-17 DNAzyme and 39E DNAzyme to develop sensors for Pb^{2+} and UO_2^{2+}. Both sensors retained high sensitivity and selectivity [179,180].

Another label-free fluorescence sensor was reported by Zhang et al. utilizing the double-stranded DNA chelating dye Picogreen and the 17E DNAzyme for the detection of Pb^{2+}. The dye binds to double-stranded DNA in the absence of Pb^{2+}, producing a high fluorescence state; after addition of Pb^{2+}, catalytic cleavage of the substrate causes dissociation of the enzyme-substrate complex, releasing the chelated dye and reducing the overall fluorescence. Because of the "turn-off" nature of this system, a higher detection limit of 10 nM is reported when compared to the ATMND system [181].

5.2 Colorimetric Sensors

Although fluorescence sensors can offer high sensitivity and selectivity for detection, they still require instruments for signal output. Even a small portable fluorometer can be a limitation for on-site and real-time detection because of cost issues. Colorimetry is ideal for its convenience because the presence of the analyte can be seen directly by a color change. Metallic nanoparticles, especially gold nanoparticles (AuNPs), display strong distance-dependent optical properties and very high extinction coefficients [182]. The change from a disperse state to an aggregate state of 13 nm AuNPs causes a color change from red to blue. Due to the polyanionic nature of DNA, aggregation of DNA-functionalized AuNPs can be prevented even in molar concentration of NaCl while bare AuNPs are less stable because of the salt-induced screening effect [183]. In addition, DNA has also been demonstrated to control the assembly or disassembly of AuNPs [184–186]. These properties have been utilized to design colorimetric sensors [182–185,187,188].

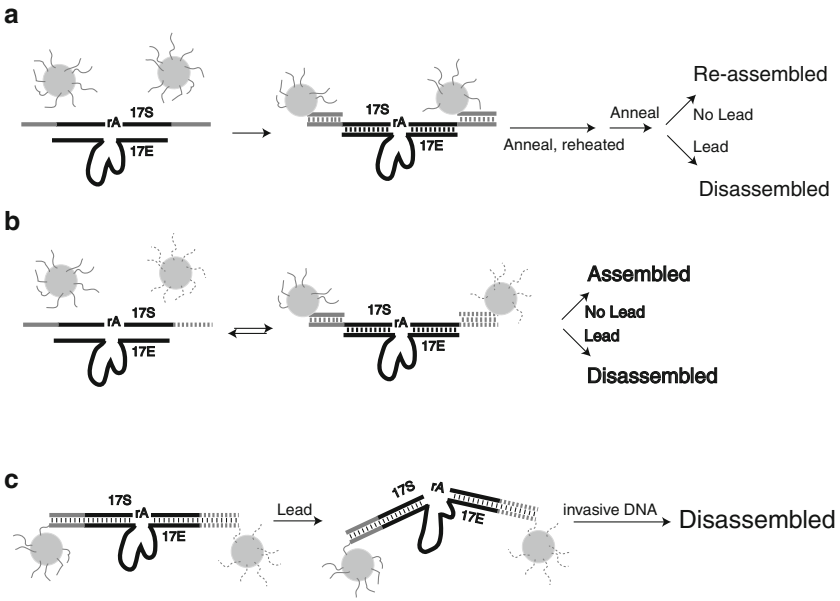

Figure 7 Designs for labelled colorimetric sensors. Grey circles denote gold nanoparticles (AuNPs). (**a**) The first colorimetric DNAzyme sensor based on the assembly and disassembly of AuNP-DNA aggregates. In this design, the AuNPs were arranged in a head-to-tail maner. (**b**) Improved design based on a head-to-head AnNP organization. (**c**) Colorimetric sensor design that utilizes an invasive DNA.

5.2.1 Labelled Colorimetric Sensors

The first colorimetric sensor for Pb^{2+} detection was based on the assembly and disassembly of gold-nanoparticles in the presence of the 8-17 DNAzyme. In this design, both substrate arms were extended and the two extended regions were designed to hybridize to their complementary strands on DNA-functionalized AuNPs (Figure 7a). In the presence of the enzyme strand, aggregate of AuNPs linked by the enzyme-substrate complex can form after a heating-and-cooling hybridization process. This DNA-AuNPs aggregate has a blue color. To perform sensing, the aggregate is heated to 50°C and then followed by a cooling process controlled by the presence of Pb^{2+}. If Pb^{2+} is present, cleavage of the substrate can prevent the formation of the blue aggregate again and a red color can be observed by spotting the sensing solution onto a TLC plate [47]. The initial colorimetric sensor required multi-step operation and long detection time; additionally, the detection limit (~100 nM) was about 50 times higher than the fluorescence sensor. Since this design was originally published, several improvements to the original sensor have been made. The heating-and-cooling process was eliminated by designing a tail-to-tail arrangement of AuNPs and the detection time was decreased to 5 minutes by increasing the size of the AuNPs used from 13 nm to 42 nm. These improvements

to the kinetics of the sensor came at the price of changing the original "turn-on" sensor to a "turn-off" sensor, since no color change can be observed in the presence of Pb^{2+} (Figure 7b) [52].

To achieve fast and "turn-on" sensing with DNAzymes, small fragments of invasive DNA have been used to assist the disassembly of the DNA-AuNPs aggregate (Figure 7c) [189,190]. Later, by using asymmetric substrate binding arms, the disassembly of the DNA-AuNPs aggregate can occur without the presence of invasive DNA at room temperature [191]. A similar design has been applied to the 39E DNAzyme to develop a UO_2^{2+} sensor [48].

Other than cleaving DNAzymes, a Cu^{2+}-dependent ligation DNAzyme has also been used for designing colorimetric sensors by similar methods. The use of a ligation DNAzyme has the advantage of an extremely low background and therefore a high sensitivity [192].

5.2.2 Label-Free Colorimetric Sensors

The colorimetric, label-free detection of an analyte is probably the most favorable method from the end user's perspective. Such a detection method is possible with DNAzymes and AuNPs. A label-free sensor employs the different absorption properties of ss- and dsDNA on citrate-coated AuNPs. Single-stranded DNA can adsorb onto AuNPs via its nucleobases and enhance the salt stability of AuNPs. Without exposed nucleobases, the negatively charged phosphate backbone of dsDNA repels the negatively charged AuNPs. Therefore, no enhanced salt stability can be observed when dsDNA is present to AuNPs [193].

Both Pb^{2+} sensors (8-17 DNAzyme) and a UO_2^{2+} sensor (39E DNAzyme) have been developed [48,49]. Since no modification is required for detection, after the addition of metal ions to the solution containing the DNAzyme and the substrate, the reaction is quenched by addition of EDTA or adjusting the pH after a period of time. Detection is performed by addition of 13 nm AuNPs to the reaction mixtures. The presence of cleaved products then can protect AuNPs from aggregating due to salts present in the reaction system and as a result, no color change is observed. Although being a "turn-off" sensor, this system can achieve very low detection limits (1 nM for UO_2^{2+} and 3 nM for Pb^{2+}). A similar label-free Pb^{2+} sensor has also been reported using bare gold nanoparticles, but with a higher detection limit of 500 nM [50].

All of the sensing methods described above require careful and accurate aliquots of small microliter amounts of solution, making it difficult for the general public with minimal scientific background or training to carry out the experiment successfully. Toward this goal, a dipstick test has been developed based on the 8-17 DNAzyme and AuNP conjugates for detection of Pb^{2+} with practical application for detecting Pb^{2+} in paints (Figure 8) [53]. In this study, the substrate carried a 3′-biotin modification and the 5′-end was extended with a thiol group. The substrate was conjugated to the AuNPs via thiol-gold chemistry. The dipstick is made of four overlapping pads: the wicking pad, the conjugation pad, the lateral flow

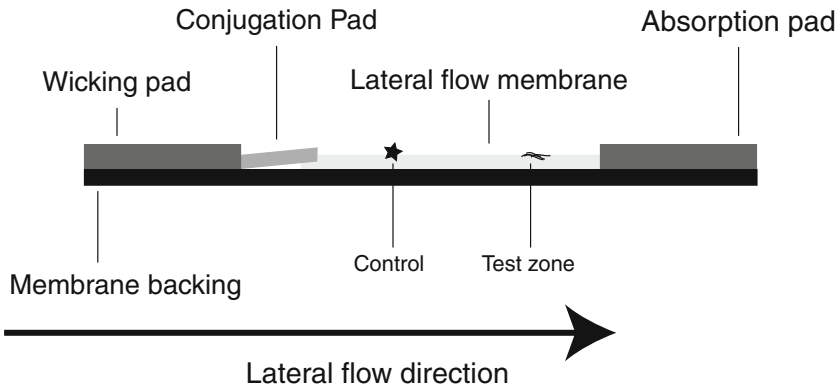

Figure 8 Design of the dipstick for lead detection. The star denotes a control line with streptavidin and the black lines at the test zone denote the capture DNA. The dipstick involved has four overlapping pads on a membrane backing. Buffer flows from the wicking pad towards the absorption pad. Uncleaved DNAzyme-substrate-AuNP conjugates are captured at the control line by streptavidin while the cleaved substrate-AuNP conjugates are captured at the test line by the capture DNA.

membrane and the absorption pad, held in place on a backing sheet. The enzyme-substrate was annealed and spotted onto the conjugation pad of the dipstick. Streptavidin was spotted on the membrane at the control zone. Capture DNA which is complimentary to the releasing part of the cleaved substrate was spotted as the test zone. After all the components dried on the membrane, the dipstick can be used for sensing. If no Pb^{2+} is present, all the DNA-AuNPs conjugates were captured by the streptavidin at the control zone, and one red line results; if Pb^{2+} is present, the cleaved substrate with the conjugated AuNPs can travel up the membrane with the buffer flow and be captured by the capture DNA. Since the cleavage reaction is generally not 100%, two lines can often be observed. With this procedure, a 5 μM detection limit is obtained. With a modified procedure, in which the reaction is carried out in solution and detection is performed on the dipstick, a 500 nM detection limit is achieved.

5.3 Electrochemical Sensors

Besides sensors with optical detections, electrochemical DNAzyme sensors have also been demonstrated. Electrochemical sensors have the advantages of high sensitivity, low cost of the electronic device detector, and convenience due to its miniaturization [79]. The first electrochemical DNAzyme sensor was reported by Xiao et al. [54]. In this study, the 8-17 DNAzyme was modified with a 3′-methylene blue (MB) group and it was 5′-thiolated. The DNAzyme was then conjugated to a gold electrode. When the substrate hybridized to the enzyme strand, the relatively rigid complex prevented

the MB group from approaching the electrode, thus preventing electron transfer. In contrast, the cleavage and release of the substrate allowed the MB to transfer electrons to the electrode. The detection limit for Pb^{2+} with this sensor was 500 nM.

Another electrochemical sensor based on the 8-17 DNAzyme was also reported but using a $[Ru(NH_3)_6]^{3+}$ and DNA-AuNPs for signal amplification [55]. The ruthenium complex can bind to the phosphate backbone of the DNA and the DNA-AuNPs hybridized to an extended region on the releasing arm of the substrate. In the absence of Pb^{2+}, electron transfer from the ruthenium complex to the electrode was maximized and amplified by the AuNPs; in the presence of Pb^{2+}, the cleaved substrate was released from the DNA-AuNPs conjugate, resulting in a reduced number of ruthenium complexes close to the electrode surface and loss of the amplification from the AuNPs. Although being a "turn-off" sensor, this sensor was still highly sensitive, demonstrating a 1 nM detection limit because of signal amplification.

5.4 Other DNAzyme Sensors

Instead of using other molecules to generate a fluorescence signal, a hemin DNAzyme (PS2.M) has also been used. This DNAzyme was first isolated as a cofactor to bind *N*-methylmesoporphyrin [92]. Later, it was found that this sequence is able to catalyze porphyrin metallation [34,94]. The hemin-DNAzyme complex has peroxidase activity, and as a result, its activity can be monitored by using common peroxidase substrates, such as luminol and ABTS [93,95,96]. The Willner group was the first to apply this DNAzyme in biosensing applications [194,195]. The strategy for using the hemin/DNAzyme complex as the signal module generally involves splitting the DNAzyme into two portions and each portion has an extension that can bind to the target [196]. In the case of a "turn-off" sensor, the presence of the trigger DNA will sterically hinder the formation of the hemin DNAzyme, and thus result in a "turn-off" state; when the trigger DNA is absent, the hemin DNAzyme is in the active state and can produce signals when luminol or ABTS is present [196]. A "turn-on" sensor was developed by first locking a portion of the hemin DNAzyme using its complimentary sequence; in the presence of the target, the fully functional DNAzyme is released and produces a signal [197–200]. More detailed reviews of this system are provided elsewhere [86].

Other than solution phase sensors, DNAzyme-based sensors can also be prepared by surface immobilization. Surface immobilization allows lower background and sensor regeneration since unhybridized and cleaved substrate can be washed away. By covalently attaching the 8-17 DNAzyme with a fluorophore-labelled substrate to a gold surface, a detection limit of 1 nM was achieved [201]. This detection limit is about ten times lower than most of the solution phase fluorescent sensors using the same DNAzyme. Besides a lower detection limit, immobilization of the DNAzyme on a gold-coated nanocapillary membrane can retain the activity of the sensor for a 30-day period at room temperature in a dried state [202,203]. Other than gold surfaces, carbon nanotubes and silica gel have also been used to immobilize and entrap DNAzyme sensors [204,205]. One step further for immobilized DNAzyme sensors

is the application in micro- and nanofluidic devices. Immobilizing DNAzyme sensors in these devices allow detection with a very small amount of materials. Generally, less than 1 nL of DNA solution is needed for sensing [44,206].

6 Concluding Remarks and Future Directions

In summary, a large number of studies have been carried out to understand the basic biochemistry of DNAzymes using the 8-17 and 10-23 DNAzymes as model systems. Many sensing applications based on these DNAzymes have been demonstrated and some of these sensors are now available commercially [207].

However, many aspects of these DNAzymes still remain to be understood, such as the nature of their metal binding site, their exact catalytic mechanisms, and most importantly, their active structures. Many more studies on these aspects will be needed to obtain a more complete picture of these DNAzymes.

The RNA-cleaving DNAzymes only represent one member of the DNAzyme family. Fundamental studies on the other DNAzymes are important to be able to understand this new class of enzymes.

Besides the basic studies on existing DNAzymes, we look forward to see more DNA catalysts, which can catalyze new types of reactions. New reactions, where the substrates are no longer nucleotides, are highly exciting, since they expand the practical application of DNAzymes into new territories.

For sensing applications, a major challenge is to apply the success of *in vitro* tests to sense and image metal ions in cells or even the human body. The study of the structure and mechanism of DNAzymes and their applications in sensing is a primary example of scientific endeavors that expand both our fundamental understanding and exploration of the frontier of practical applications. Further advances in this field will have great impacts in many areas of science, engineering, and society.

Abbreviations

ABTS	2,2′-azino-bis(3-ethylbenzthiazoline-6-sulfonic acid)
ATMND	2-amino-5,6,7-trimethyl-1,8-naphthyridine
AuNP	gold nanoparticle
CD	circular dichroism
Cy5	a cyanine dye
Dabcyl	4-(4′-dimethylaminophenylazo)benzoic acid
DNAzyme	deoxyribozyme
EDTA	ethylenediamine-N,N,N′,N′-tetraacetate
EPA	Environmental Protection Agency
FAM	6-carboxyfluorescein
FRET	Förster resonance energy transfer

hemin	Fe(III)-protoporphyrin IX
ICP-MS	inductively coupled plasma-mass spectrometry
MALDI-TOF	matrix-assisted laser desorption/ionization-time of flight
MB	methylene blue
NMR	nuclear magnetic resonance
NMM	*N*-methylmesoporphyrin
PCR	polymerase chain reaction
PAGE	polyacrylamide gel electrophoresis
QD	quantum dot
smFRET	single molecule Förster resonance energy transfer
ssDNA	single-stranded DNA
TLC	thin layer chromatography
TMR = TAMRA	6-carboxytetramethylrhodamine

Acknowledgments The research of the Lu group described in this chapter has been generously supported by the U.S. Department of Energy, the National Institutes of Health, the Department of Defense, the Department of Housing and Urban Development, the Environmental Protection Agency, the National Science Foundation, and the Illinois Sustainable Technology Center.

References

1. K. Kruger, P. J. Grabowski, A. J. Zaug, J. Sands, D. E. Gottschling, T. R. Cech, *Cell* **1982**, *31*, 147–157.
2. C. Guerrier-Takada, K. Gardiner, T. Marsh, N. Pace, S. Altman, *Cell* **1983**, *35*, 849–857.
3. R. R. Breaker, G. F. Joyce, *Chem. Biol*. **1994**, *1*, 223–229.
4. S. W. Santoro, G. F. Joyce, *Proc. Natl. Acad. Sci. USA* **1997**, *94*, 4262–4266.
5. J. Li, W. Zheng, A. H. Kwon, Y. Lu, *Nucleic Acids Res*. **2000**, *28*, 481–488.
6. C. R. Geyer, D. Sen, *Chem. Biol*. **1997**, *4*, 579–593.
7. D. Faulhammer, M. Famulok, *Angew. Chem., Int. Ed. Engl*. **1996**, *35*, 2837–2841.
8. A. R. Feldman, D. Sen, *J. Mol. Biol*. **2001**, *313*, 283–294.
9. R. P. G. Cruz, J. B. Withers, Y. Li, *Chem. Biol*. **2004**, *11*, 57–67.
10. J. Liu, A. K. Brown, X. Meng, D. M. Cropek, J. D. Istok, D. B. Watson, Y. Lu, *Proc. Natl. Acad. Sci. USA* **2007**, *104*, 2056–2061.
11. N. Carmi, L. A. Shultz, R. R. Breaker, *Chem. Biol*. **1996**, *3*, 1039–1046.
12. N. Carmi, H. R. Balkhi, R. R. Breaker, *Proc. Natl. Acad. Sci. USA* **1998**, *95*, 2233–2237.
13. N. Carmi, R. R. Breaker, *Bioorg. Med. Chem*. **2001**, *9*, 2589–2600.
14. M. Chandra, A. Sachdeva, S. K. Silverman, *Nat. Chem. Biol*. **2009**, *5*, 718–720.
15. Y. Xiao, M. Chandra, S. K. Silverman, *Biochemistry* **2010**.
16. Y. Xiao, E. C. Allen, S. K. Silverman, *Chem. Commun*. **2011**, *47*, 1749–1751.
17. J. Burmeister, G. von Kiedrowski, A. D. Ellington, *Angew. Chem., Int. Ed. Engl*. **1997**, *36*, 1321–1324.
18. B. Cuenoud, J. W. Szostak, *Nature* **1995**, *375*, 611–614.
19. A. Sreedhara, Y. Li, R. R. Breaker, *J. Am. Chem. Soc*. **2004**, *126*, 3454–3460.
20. R. L. Coppins, W. E. Purtha, Y. Wang, S. K. Silverman "Synthesis of native 3'-5' RNA linkages by deoxyribozymes", *229th ACS National Meeting*, San Diego, CA, USA, 2005, ORGN–653.
21. W. E. Purtha, R. L. Coppins, M. K. Smalley, S. K. Silverman, *J. Am. Chem. Soc*. **2005**, *127*, 13124–13125.
22. Y. Wang, S. K. Silverman, *Biochemistry* **2003**, *42*, 15252–15263.

23. Y. Wang, S. K. Silverman, *J. Am. Chem. Soc*. **2003**, *125*, 6880–6881.
24. R. L. Coppins, S. K. Silverman, *Nat. Struct. Mol. Biol*. **2004**, *11*, 270–274.
25. R. L. Coppins, S. K. Silverman, *J. Am. Chem. Soc*. **2005**, *127*, 2900–2907.
26. E. D. Pratico, Y. Wang, S. K. Silverman, *Nucleic Acids Res*. **2005**, *33*, 3503–3512.
27. Y. Wang, S. K. Silverman, *Angew. Chem., Int. Ed. Engl*. **2005**, *44*, 5863–5866.
28. P. I. Pradeepkumar, C. Hoebartner, D. A. Baum, S. K. Silverman, *Angew. Chem., Int. Ed. Engl.* **2008**, *47*, 1753–1757.
29. W. Wang, L. P. Billen, Y. Li, *Chem. Biol*. **2002**, *9*, 507–517.
30. Y. Li, Y. Liu, R. R. Breaker, *Biochemistry* **2000**, *39*, 3106–3114.
31. C. Höbartner, P. I. Pradeepkumar, S. K. Silverman, *Chem. Commun.* **2007**, 2255–2257.
32. T. L. Sheppard, P. Ordoukhanian, G. F. Joyce, *Proc. Natl. Acad. Sci. USA* **2000**, *97*, 7802–7807.
33. M. Chandra, S. K. Silverman, *J. Am. Chem. Soc*. **2008**, *130*, 2936–2937.
34. Y. Li, D. Sen, *Nat. Struct. Biol*. **1996**, *3*, 743–747.
35. Y. Li, D. Sen, *Biochemistry* **1997**, *36*, 5589–5599.
36. T. Lan, K. Furuya, Y. Lu, *Chem. Commun*. **2010**, *46*, 3896–3898.
37. A. K. Brown, J. Liu, Y. He, Y. Lu, *ChemBioChem* **2009**, *10*, 486–492.
38. J. Li, Y. Lu, *J. Am. Chem. Soc*. **2000**, *122*, 10466–10467.
39. J. Liu, Y. Lu, *Anal. Chem*. **2003**, *75*, 6666–6672.
40. N. Nagraj, J. Liu, S. Sterling, J. Wu, Y. Lu, *Chem. Commun.* **2009**, 4103–4105.
41. J. Liu, Y. Lu, *Angew. Chem., Int. Ed. Engl*. **2007**, *46*, 7587–7590.
42. J. Liu, Y. Lu, *J. Am. Chem. Soc*. **2007**, *129*, 9838–9839.
43. T. S. Dalavoy, D. P. Wernette, M. Gong, J. V. Sweedler, Y. Lu, B. R. Flachsbart, M. A. Shannon, P. W. Bohn, D. M. Cropek, *Lab Chip* **2008**, *8*, 786–793.
44. I.-H. Chang, J. J. Tulock, J. Liu, W.-S. Kim, D. M. Cannon, Jr., Y. Lu, P. W. Bohn, J. V. Sweedler, D. M. Cropek, *Environ. Sci. Technol*. **2005**, *39*, 3756–3761.
45. T. Li, S. Dong, E. Wang, *J. Am. Chem. Soc*. **2010**, *132*, 13156–13157.
46. X. B. Zhang, Z. Wang, H. Xing, Y. Xiang, Y. Lu, *Anal. Chem*. **2010**, *82*, 5005–5011.
47. J. Liu, Y. Lu, *J. Am. Chem. Soc*. **2003**, *125*, 6642–6643.
48. J. H. Lee, Z. Wang, J. Liu, Y. Lu, *J. Am. Chem. Soc*. **2008**, *130*, 14217–14226.
49. Z. Wang, J. H. Lee, Y. Lu, *Adv. Mater*. **2008**, *20*, 3263–3267.
50. H. Wei, B. Li, J. Li, S. Dong, E. Wang, *Nanotechnology* **2008**, *19*, 095501–095505.
51. J. W. Liu, Y. Lu, *J. Fluoresc*. **2004**, *14*, 343–354.
52. J. Liu, Y. Lu, *Chem. Mater*. **2004**, *16*, 3231–3238.
53. D. Mazumdar, J. Liu, G. Lu, J. Zhou, Y. Lu, *Chem. Commun*. **2009**, *46*, 1416–1418.
54. Y. Xiao, A. A. Rowe, K. W. Plaxco, *J. Am. Chem. Soc*. **2007**, *129*, 262–263.
55. L. Shen, Z. Chen, Y. Li, S. He, S. Xie, X. Xu, Z. Liang, X. Meng, Q. Li, Z. Zhu, M. Li, X. C. Le, Y. Shao, *Anal. Chem*. **2008**, *80*, 6323–6328.
56. D. A. Baum, S. K. Silverman, *Cell. Mol. Life Sci*. **2008**, *65*, 2156–2174.
57. C. R. Dass, P. F. Choong, L. M. Khachigian, *Mol. Cancer. Ther*. **2008**, *7*, 243–251.
58. S. Chakraborti, A. C. Banerjea, *Mol. Ther*. **2003**, *7*, 817–826.
59. R. Goila, A. C. Banerjea, *Biochem. J*. **2001**, *353*, 701–708.
60. S. W. Santoro, in *Synthetic Nucleic Acids as Inhibitors of Gene Expression*, Ed L. M. Khachigian, CRC Press, Boca Raton, 2005, pp. 53–68.
61. T. Toyoda, Y. Imamura, H. Takaku, T. Kashiwagi, K. Hara, J. Iwahashi, Y. Ohtsu, N. Tsumura, H. Kato, N. Hamada, *FEBS Lett*. **2000**, *481*, 113–116.
62. J. Nowakowski, P. J. Shim, G. F. Joyce, C. D. Stout, *Acta Crystallogr. D. Biol. Crystallogr*. **1999**, *D55*, 1885–1892.
63. J. Nowakowski, P. J. Shim, G. S. Prasad, C. D. Stout, G. F. Joyce, *Nat. Struct. Biol*. **1999**, *6*, 151–156.
64. C. Tuerk, L. Gold, *Science* **1990**, *249*, 505–510.
65. A. D. Ellington, J. W. Szostak, *Nature* **1990**, *346*, 818–822.
66. A. A. Beaudry, G. F. Joyce, *Science* **1992**, *257*, 635–641.
67. M. Zuker, *Nucleic Acids Res*. **2003**, *31*, 3406–3415.

68. A. K. Brown, J. Li, C. M. B. Pavot, Y. Lu, *Biochemistry* **2003**, *42*, 7152–7161.
69. S. W. Santoro, G. F. Joyce, *Biochemistry* **1998**, *37*, 13330–13342.
70. A. Peracchi, *J. Biol. Chem*. **2000**, *275*, 11693–11697.
71. Q.-C. He, J.-M. Zhou, D.-M. Zhou, Y. Nakamatsu, T. Baba, K. Taira, *Biomacromolecules* **2002**, *3*, 69–83.
72. R. R. Breaker, G. M. Emilsson, D. Lazarev, S. Nakamura, I. J. Puskarz, A. Roth, N. Sudarsan, *RNA* **2003**, *9*, 949–957.
73. G. M. Emilsson, S. Nakamura, A. Roth, R. R. Breaker, *RNA* **2003**, *9*, 907–918.
74. K. Schlosser, Y. Li, *Biochemistry* **2004**, *43*, 9695–9707.
75. K. Schlosser, J. Gu, L. Sule, Y. Li, *Nucleic Acids Res*. **2008**, *36*, 1472–1481.
76. K. Schlosser, Y. Li, *ChemBioChem* **2010**, *11*, 866–879.
77. S. Sando, T. Sasaki, K. Kanatani, Y. Aoyama, *J. Am. Chem. Soc*. **2003**, *125*, 15720–15721.
78. S. Sando, A. Narita, T. Sasaki, Y. Aoyama, *Org. Biomol. Chem*. **2005**, *3*, 1002–1007.
79. J. Liu, Z. Cao, Y. Lu, *Chem. Rev*. **2009**, *109*, 1948–1998.
80. X. Zhang, R. Kong, Y. Lu, *Annu. Rev. Anal. Chem.* **2011**, *4*, DOI: 10.1146/annurev.anchem.111808.073617.
81. Y. Lu, J. Liu, J. Li, P. J. Bruesehoff, C. M. B. Pavot, A. K. Brown, *Biosens. Bioelectron*. **2003**, *18*, 529–540.
82. M. N. Stojanovic, T. E. Mitchell, D. Stefanovic, *J. Am. Chem. Soc*. **2002**, *124*, 3555–3561.
83. M. N. Stojanovic, D. Stefanovic, *J. Am. Chem. Soc*. **2003**, *125*, 6673–6676.
84. M. N. Stojanovic, S. Semova, D. Kolpashchikov, J. Macdonald, C. Morgan, D. Stefanovic, *J. Am. Chem. Soc*. **2005**, *127*, 6914–6915.
85. H. Lederman, J. Macdonald, D. Stefanovic, M. N. Stojanovic, *Biochemistry* **2006**, *45*, 1194–1199.
86. I. Willner, B. Shlyahovsky, M. Zayats, B. Willner, *Chem. Soc. Rev*. **2008**, *37*, 1153–1165.
87. J. Elbaz, O. Lioubashevski, F. Wang, F. Remacle, R. D. Levine, I. Willner, *Nature Nanotech*. **2010**, *5*, 417–422.
88. A. Flynn-Charlebois, Y. Wang, T. K. Prior, I. Rashid, K. A. Hoadley, R. L. Coppins, A. C. Wolf, S. K. Silverman, *J. Am. Chem. Soc*. **2003**, *125*, 2444–2454.
89. A. Flynn-Charlebois, T. K. Prior, K. A. Hoadley, S. K. Silverman, *J. Am. Chem. Soc*. **2003**, *125*, 5346–5350.
90. Y. Wang, S. K. Silverman, *Biochemistry* **2005**, *44*, 3017–3023.
91. C. Hobartner, S. K. Silverman, *Biopolymers* **2007**, *87*, 279–292.
92. Y. Li, C. R. Geyer, D. Sen, *Biochemistry* **1996**, *35*, 6911–6922.
93. P. Travascio, Y. Li, D. Sen, *Chem. Biol*. **1998**, *5*, 505–517.
94. P. Travascio, A. J. Bennet, D. Y. Wang, D. Sen, *Chem. Biol*. **1999**, *6*, 779–787.
95. P. Travascio, D. Sen, A. J. Bennet, *Can. J. Chem*. **2006**, *84*, 613–619.
96. H.-W. Lee, D. J. F. Chinnapen, D. Sen, *Pure Appl. Chem*. **2004**, *76*, 1537–1545.
97. B. Seelig, A. Jaschke, *Chem.Biol*. **1999**, *6*, 167–176.
98. N. Sugimoto, Y. Okumoto, T. Ohmichi, *J. Chem. Soc., Perkin Trans. 2* **1999**, 1381–1386.
99. Z. Zaborowska, J. P. Fuerste, V. A. Erdmann, J. Kurreck, *J. Biol. Chem*. **2002**, *277*, 40617–40622.
100. Z. Zaborowska, S. Schubert, J. Kurreck, V. A. Erdmann, *FEBS Lett*. **2004**, *579*, 554–558.
101. G. F. Joyce, *Methods Enzymol*. **2001**, *341*, 503–517.
102. A. Peracchi, M. Bonaccio, M. Clerici, *J. Mol. Biol*. **2005**, *352*, 783–794.
103. B. Wang, L. Cao, W. Chiuman, Y. Li, Z. Xi, *Biochemistry* **2010**, *49*, 7553–7562.
104. Y. Liu, D. Sen, *J. Mol. Biol*. **2008**, *381*, 845–859.
105. Y. Liu, D. Sen, *J. Mol. Biol*. **2010**, *395*, 234.
106. G. S. Sekhon, D. Sen, *Biochemistry* **2010**, *49*, 9072–9077.
107. C. J. Burrows, J. G. Muller, *Chem. Rev*. **1998**, *98*, 1109–1151.
108. H. K. Kim, J. Liu, J. Li, N. Nagraj, M. Li, C. M. B. Pavot, Y. Lu, *J. Am. Chem. Soc*. **2007**, *129*, 6896–6902.
109. H. K. Kim, I. Rasnik, J. Liu, T. Ha, Y. Lu, *Nat. Chem. Biol*. **2007**, *3*, 763–768.

110. E. K. Y. Leung, D. Sen, *Chem. Biol*. **2007**, *14*, 41–51.
111. D. Faulhammer, M. Famulok, *J. Mol. Biol*. **1997**, *269*, 188–202.
112. K. Schlosser, J. Gu, J. C. Lam, Y. Li, *Nucleic Acids Res*. **2008**, *36*, 4768–4777.
113. M. Bonaccio, A. Credali, A. Peracchi, *Nucleic Acids Res*. **2004**, *32*, 916–925.
114. K. Schlosser, Y. Li, *Nucleic Acids Res*. **2009**, *37*, 413–420.
115. J. A. Cowan, *J. Inorg. Biochem*. **1993**, *49*, 171–175.
116. D. Mazumdar, N. Nagraj, H. K. Kim, X. Meng, A. K. Brown, Q. Sun, W. Li, Y. Lu, *J. Am. Chem. Soc*. **2009**, *131*, 5506–5515.
117. B. Nawrot, K. Widera, M. Wojcik, B. Rebowska, G. Nowak, W. J. Stec, *FEBS Lett*. **2007**, *274*, 1062–1072.
118. R. M. Clegg, *Methods Enzymol*. **1992**, *211*, 353–388.
119. M. Lorenz, A. Hillisch, S. Diekmann, *Rev. Mol. Biotechnol*. **2002**, *82*, 197–209.
120. D. M. J. Lilley, T. J. Wilson, *Curr. Opin. Chem. Biol*. **2000**, *4*, 507–517.
121. N. G. Walter, *Methods* **2001**, *25*, 19–30.
122. C. Gohlke, A. I. H. Murchie, D. M. J. Lilley, R. M. Clegg, *Proc. Natl. Acad. Sci. USA* **1994**, *91*, 11660–11664.
123. F. Stuehmeier, J. B. Welch, A. I. H. Murchie, D. M. J. Lilley, R. M. Clegg, *Biochemistry* **1997**, *36*, 13530–13538.
124. R. M. Clegg, A. I. H. Murchie, D. M. J. Lilley, *Biophys. J*. **1994**, *66*, 99–109.
125. G. S. Bassi, A. I. H. Murchie, F. Walter, R. M. Clegg, D. M. J. Lilley, *EMBO J*. **1997**, *16*, 7481–7489.
126. J. B. Murray, A. A. Seyhan, N. G. Walter, J. M. Burke, W. G. Scott, *Chem. Biol*. **1998**, *5*, 587–595.
127. N. G. Walter, J. M. Burke, D. P. Millar, *Nat. Struct. Biol*. **1999**, *6*, 544–549.
128. K. J. Hampel, J. M. Burke, *Biochemistry* **2001**, *40*, 3723–3729.
129. M. J. B. Pereira, D. A. Harris, D. Rueda, N. G. Walter, *Biochemistry* **2002**, *41*, 730–740.
130. A. Jenne, W. Gmelin, N. Raffler, M. Famulok, *Angew.Chem., Int. Ed*. **1999**, *38*, 1300–1303.
131. X.-w. Fang, T. Pan, T. R. Sosnick, *Nat. Struct. Biol*. **1999**, *6*, 1091–1095.
132. M. I. Wallace, L. Ying, S. Balasubramanian, D. Klenerman, *Proc. Natl. Acad. Sci. USA* **2001**, *98*, 5584–5589.
133. K. M. Parkhurst, M. Brenowitz, L. J. Parkhurst, *Biochemistry* **1996**, *35*, 7459–7465.
134. V. V. Didenko, *BioTechniques* **2001**, *31*, 1106–1121.
135. J. Liu, Y. Lu, *J. Am. Chem. Soc*. **2002**, *124*, 15208–15216.
136. W. H. Sawyer, R. Y. S. Chan, J. F. Eccleston, B. E. Davidson, S. A. Samat, Y. Yan, *Biochemistry* **2000**, *39*, 5653–5661.
137. A. Bhattacharyya, B. Bhattacharyya, S. Roy, *Eur. J. Biochem*. **1993**, *216*, 757–761.
138. A. K. Tong, S. Jockusch, Z. Li, H.–R. Zhu, D. L. Akins, N. J. Turro, J. Ju, *J. Am. Chem. Soc*. **2001**, *123*, 12923–12924.
139. J. C. F. Lam, Y. Li, *ChemBioChem* **2010**, *11*, 1710–1719.
140. N. K. Lee, H. R. Koh, K. Y. Han, S. K. Kim, *J. Am. Chem. Soc*. **2007**, *129*, 15526–15534.
141. N. K. Lee, H. R. Koh, K. Y. Han, J. Lee, S. K. Kim, *Chem. Commun*. **2010**, *46*, 4683–4685.
142. Y.-J. Choi, H.-J. Han, J.-H. Lee, S.-W. Suh, B.-S. Choi, *Bull. Korean Chem. Soc*. **2000**, *21*, 955–956.
143. D. E. Draper, *Biophys.Chem*. **1985**, *21*, 91–101.
144. A. L. Feig, W. G. Scott, O. C. Uhlenbeck, *Science* **1998**, *279*, 81–84.
145. A. L. Feig, M. Panek, W. D. Horrocks, Jr., O. C. Uhlenbeck, *Chem. Biol*. **1999**, *6*, 801–810.
146. D. S. Gross, H. Simpkins, *J. Biol. Chem*. **1981**, *256*, 9593–9598.
147. M. D. Topal, J. R. Fresco, *Biochemistry* **1980**, *19*, 5531–5537.
148. R. K. O. Sigel, A. M. Pyle, *Met. Ions Biol. Syst*. **2003**, *40*, 477–512.
149. N. L. Greenbaum, C. Mundoma, D. R. Peterman, *Biochemistry* **2001**, *40*, 1124–1134.
150. H. K. Kim, J. Li, N. Nagraj, Y. Lu, *Chem. Eur. J*. **2008**, *232*, 8696.
151. C. R. Geyer, D. Sen, *J. Mol. Biol*. **1998**, *275*, 483–489.
152. F. M. Pohl, T. M. Jovin, *J. Mol. Biol*. **1972**, *67*, 375–396.

153. T. J. Thamann, R. C. Lord, A. H. Wang, A. Rich, *Nucleic Acids Res*. **1981**, *9*, 5443–5457.
154. M. W. Germann, K. H. Schoenwaelder, J. H. Van de Sande, *Biochemistry* **1985**, *24*, 5698–5702.
155. Y. Wang, G. A. Thomas, W. L. Peticolas, *Biochemistry* **1987**, *26*, 5178–5186.
156. L. E. Xodo, G. Manzini, F. Quadrifoglio, G. A. Van der Marel, J. H. Van Boom, *Biochemistry* **1988**, *27*, 6327–6331.
157. B. Hernandez, V. Baumruk, C. Gouyette, M. Ghomi, *Biopolymers* **2005**, *78*, 21–34.
158. M. Cieslak, J. Szymanski, R. W. Adamiak, C. S. Cierniewski, *J. Biol. Chem*. **2003**, *278*, 47987–47996.
159. G. W. Ewing, *Analytical Instrumentation Handbook*, M. Dekker, New York, 1997.
160. R. Y. Tsien, A. W. Czarnik, in *Fluorescenct Chemosensors for Ion and Molecule Recognization*, Vol. 538 of *ACS Symposium Series*, Ed A. W. Czarnik, American Chemical Society, Washington, DC, 1993, pp. 130–146.
161. A. W. Czarnik, *Chem. Biol*. **1995**, *2*, 423–428.
162. A. W. Czarnik, *Acc. Chem. Res*. **1994**, *27*, 302–308.
163. K. Schlosser, S. A. McManus, Y. Li, in *The Aptamer Handbook: Functional Oligonucleotides and Their Applications*, Ed S. Klussmann, Wiley-VCH, Weinheim, 2006, pp. 228–261.
164. *Functional Nucleic Acids for Sensing and Other Analytical Applications*, Vol. 8 of *Integrated Analytical Systems*, Eds Y. Li, Y. Lu, Springer, New York, 2009.
165. S. K. Silverman, *Chem. Commun*. **2008**, *30*, 3467–3485.
166. S. K. Silverman, *Acc. Chem. Res*. **2009**, *42*, 1521–1531.
167. Y. Lu, *Chem. Eur. J*. **2002**, *8*, 4589–4596.
168. H. Wang, Y. Kim, H. Liu, Z. Zhu, S. Bamrungsap, W. Tan, *J. Am. Chem. Soc*. **2009**, *131*, 8221–8226.
169. D. W. Boomer, M. J. Powell, *Anal. Chem*. **1987**, *59*, 2810–2813.
170. W. Chiuman, Y. Li, *Nucleic Acids Res*. **2007**, *35*, 401–405.
171. S. H. J. Mei, Z. Liu, J. D. Brennan, Y. Li, *J. Am. Chem. Soc*. **2003**, *125*, 412–420.
172. Z. Liu, S. H. J. Mei, J. D. Brennan, Y. Li, *J. Am. Chem. Soc*. **2003**, *125*, 7539–7545.
173. S. Hohng, T. Ha, *ChemPhysChem* **2005**, *6*, 956–960.
174. D. M. Willard, A. Van Orden, *Nature Mater*. **2003**, *2*, 575–576.
175. C. S. Wu, M. K. Khaing Oo, X. Fan, *ACS Nano* **2010**, *4*, 5897–5904.
176. R. A. Reynolds, III, C. A. Mirkin, R. L. Letsinger, *J. Am. Chem. Soc*. **2000**, *122*, 3795–3796.
177. J. Yguerabide, E. E. Yguerabide, *Anal. Biochem*. **1998**, *262*, 137–156.
178. J. H. Kim, S. H. Han, B. H. Chung, *Biosens. Bioelectron*. **2011**, *26*, 2125–2129.
179. Y. Xiang, A. Tong, Y. Lu, *J. Am. Chem. Soc*. **2009**, *131*, 15352–15357.
180. Y. Xiang, Z. Wang, H. Xing, N. Y. Wong, Y. Lu, *Anal. Chem*. **2010**, *82*, 4122–4129.
181. L. Zhang, B. Han, T. Li, E. Wang, *Chem. Commun*. **2011**, *47*, 3099–3101.
182. J. Liu, Y. Lu, *Nat. Protoc*. **2006**, *1*, 246–252.
183. I. I. Lim, W. Ip, E. Crew, P. N. Njoki, D. Mott, C. J. Zhong, Y. Pan, S. Zhou, *Langmuir* **2007**, *23*, 826–833.
184. C. A. Mirkin, R. L. Letsinger, R. C. Mucic, J. J. Storhoff, *Nature* **1996**, *382*, 607–609.
185. J. J. Storhoff, A. A. Lazarides, R. C. Mucic, C. A. Mirkin, R. L. Letsinger, G. C. Schatz, *J. Am. Chem. Soc*. **2000**, *122*, 4640–4650.
186. H. Li, L. Rothberg, *Proc. Natl. Acad. Sci. USA* **2004**, *101*, 14036–14039.
187. W. Zhao, F. Gonzaga, Y. Li, M. A. Brook, *Adv. Mater*. **2007**, *19*, 1766–1771.
188. K. Sato, K. Hosokawa, M. Maeda, *J. Am. Chem. Soc*. **2003**, *125*, 8102–8103.
189. J. Liu, Y. Lu, *J. Am. Chem. Soc*. **2004**, *126*, 12298–12305.
190. J. Liu, D. P. Wernette, Y. Lu, *Angew. Chem., Int. Ed. Engl*. **2005**, *44*, 7290–7293.
191. J. Liu, Y. Lu, *Org. Biomol. Chem*. **2006**, *4*, 3435–3441.
192. J. Liu, Y. Lu, *Chem. Commun.* **2007**, 4872–4874.
193. H. Li, L. J. Rothberg, *J. Am. Chem. Soc*. **2004**, *126*, 10958–10961.
194. I. Willner, R. Baron, B. Willner, *Biosens. Bioelectron*. **2007**, *22*, 1841–1852.
195. I. Willner, B. Willner, E. Katz, *Bioelectrochemistry* **2007**, *70*, 2–11.
196. Y. Xiao, V. Pavlov, R. Gill, T. Bourenko, I. Willner, *ChemBioChem* **2004**, *5*, 374–379.

197. T. Niazov, V. Pavlov, Y. Xiao, R. Gill, I. Willner, *Nano Letters* **2004**, *4*, 1683–1687.
198. V. Pavlov, Y. Xiao, R. Gill, A. Dishon, M. Kotler, I. Willner, *Anal. Chem*. **2004**, *76*, 2152–2156.
199. Y. Xiao, V. Pavlov, T. Niazov, A. Dishon, M. Kotler, I. Willner, *J. Am. Chem. Soc*. **2004**, *126*, 7430–7431.
200. J. Elbaz, M. Moshe, B. Shlyahovsky, I. Willner, *Chem. Eur. J*. **2009**, *15*, 3411–3418.
201. C. B. Swearingen, D. P. Wernette, D. M. Cropek, Y. Lu, J. V. Sweedler, P. W. Bohn, *Anal. Chem*. **2005**, *77*, 442–448.
202. D. P. Wernette, C. B. Swearingen, D. M. Cropek, Y. Lu, J. V. Sweedler, P. W. Bohn, *Analyst* **2006**, *131*, 41–47.
203. D. P. Wernette, C. Mead, P. W. Bohn, Y. Lu, *Langmuir* **2007**, *23*, 9513–9521.
204. T.-J. Yim, J. Liu, Y. Lu, R. S. Kane, J. S. Dordick, *J. Am. Chem. Soc*. **2005**, *127*, 12200–12201.
205. Y. Shen, G. Mackey, N. Rupcich, D. Gloster, W. Chiuman, Y. Li, J. D. Brennan, *Anal. Chem*. **2007**, *79*, 3494–3503.
206. A. K. Shaikh, K. S. Ryu, E. D. Goluch, J.-M. Nam, J. Liu, C. S. Thaxton, N. T. Chiesl, A. E. Barron, Y. Lu, C. A. Mirkin, C. Liu, *Proc. Natl. Acad. Sci. USA* **2005**, *102*, 9745–9750.
207. ANDalyze, Inc., 2010, http://www.andalyze.com. (accessed on April 8, 2011).